ARTICLE
Journal of Cellular Biochemistry 111:1453–1463 (2010)

Journal of Cellular Biochemistry

Anti-Fibrotic Effect of Chorionic Plate-derived Mesenchymal Stem Cells Isolated from Human Placenta in a Rat Model of CCl_4-injured Liver: Potential Application to the Treatment of Hepatic Diseases

Min-Jae Lee,[1] Jieun Jung,[2] Kyu-Hwan Na,[2] Ji Suk Moon,[2] Hey-Jin Lee,[3] Jae-Hwan Kim,[2] Gwang Il Kim,[4] Sung-Won Kwon,[5] Seong-Gyu Hwang,[6*] and Gi Jin Kim[2*]

[1] *School of Veterinary Medicine, Kangwon National University, Chuncheon, Kangwon-do, Republic of Korea*
[2] *Department of Biomedical Science, CHA University, Seoul, Republic of Korea*
[3] *ChaBio and Diostech Co., Ltd., CHA Stem Cell Institute, Seoul, Republic of Korea*
[4] *Department of Pathology, CHA Bundang Medical Center, CHA University, Seongnam, Republic of Korea*
[5] *Department of Surgery, CHA Bundang Medical Center, CHA University, Seongnam, Republic of Korea*
[6] *Department of Internal Medicine, CHA Bundang Medical Center, CHA University, Seongnam, Republic of Korea*

ABSTRACT

Translational studies have explored the therapeutic effects of stem cells, raising hopes for the treatment of numerous diseases. Here, we evaluated the therapeutic effect of chorionic plate-derived mesenchymal stem cells (CP-MSCs) isolated from human placenta and transplanted into rats with carbon tetrachloride (CCl_4)-injured livers. CP-MSCs were analyzed for hepatocyte-specific gene expression, indocyanine green (ICG) uptake, glycogen storage, and urea production following hepatogenic differentiation. PKH26-labeled CP-MSCs were directly transplanted into the livers of rats that had been exposed to CCl_4 (1.6 g/kg, twice per week for 9 weeks). Blood and liver tissue were analyzed at 1, 2, and 3 weeks post-transplantation. The expression of type I collagen (Col I) and matrix metalloproteinases (MMPs) was analyzed in rat T-HSC/Cl-6 hepatic stellate cells co-cultured with CP-MSCs following exposure to TGF-β. The expression levels of α-smooth muscle actin (α-SMA) and Col I were lower in transplanted (TP) rats than in non-transplanted (Non-TP) animals ($P < 0.05$), whereas the expression levels of albumin and MMP-9 were increased. TP rats exhibited significantly higher uptake/excretion of ICG than non-TP rats ($P < 0.005$). In addition, collagen synthesis in T-HSC/Cl-6 cells exposed to TGF-β was decreased by co-culture with CP-MSCs, which triggered the activation of MMP-2 and MMP-9. These results contribute to our understanding of the potential pathophysiological roles of CP-MSCs, including anti-fibrotic effects in liver disease, and provide a foundation for the development of new cell therapy-based strategies for the treatment of difficult-to-treat liver diseases. J. Cell. Biochem. 111: 1453–1463, 2010.

KEY WORDS: CHORIONIC PLATE-DERIVED MESENCHYMAL STEM CELLS; HEPATIC FAILURE; TRANSPLANTATION; ANTI-FIBROTIC EFFECT; COLLAGEN SYNTHESIS

Liver diseases are among the most common medical problems in Southeast Asia [Di Bisceglie et al., 1998]. The endpoint of progressive damage to the liver is loss of 80–90% of hepatic functional capacity. Ultimately, mortality from hepatic failure occurs in 70–95% of patients [JM, 1999]. While transplantation is currently an accepted therapy for liver disease, there remain many challenges to overcome in clinical practice, which is limited by a shortage of donors and the harshness of the invasive procedures

Seong-Gyu Hwang and Gi Jin Kim contributed equally to this work.

Grant sponsor: The Korea Healthcare technology R&D Project, Ministry for Health Welfare & Family Affairs, Republic of Korea A084633.

*Correspondence to: Seong-Gyu Hwang, MD, Department of Internal Medicine, CHA Bundang Medical Center, CHA University, 351 Yatap-dong, Bundang-gu, Seongnam 463-712, Republic of Korea. E-mail: sghwang@cha.ac.kr

*Correspondence to: Prof. Gi Jin Kim, PhD, Department of Biomedical Science, CHA University, 606-16 Yeoksam 1-dong, Kangnam-ku, Seoul 135-081, Republic of Korea. E-mail: gjkim@cha.ac.kr

Received 4 June 2010; Accepted 30 August 2010 • DOI 10.1002/jcb.22873 • © 2010 Wiley-Liss, Inc.
Published online 9 September 2010 in Wiley Online Library (wileyonlinelibrary.com).

[Berg et al., 2007; Perkins, 2007]. Thus, new therapies and novel strategies are required for the treatment of severe cases of hepatic dysfunction.

Several reports have demonstrated the capacity of bone marrow-derived mesenchymal stem cells (BM-MSCs) to differentiate into hepatocyte-like cells, as well as their ability to reduce chronic fibrogenesis [Sakaida et al., 2004; Zhao et al., 2005; Oyagi et al., 2006]. In addition, Jung et al. [2009] reported that human umbilical cord blood-derived mesenchymal stem cells ameliorated liver fibrosis in rats with carbon tetrachloride (CCl_4)-induced cirrhosis. However, these results are controversial, as they vary somewhat across different animal models, CCl_4 treatment protocols, and in vitro conditions [Zhao et al., 2005; Oyagi et al., 2006]. Although BM-MSCs represent an attractive therapeutic candidate for treating degenerative diseases, their use is limited by several factors, including low cell yields from donor BM, dependence on donor age, limitations to autologous use, and difficulty in recruiting donors [Costa and Grayson, 1991; Huttmann et al., 2003; Sakaida et al., 2004; Stolzing et al., 2008].

Placenta-derived stem cells (PDSCs), which have received much research attention, exhibit characteristics similar to those of BM-MSCs, but they enjoy several advantages [Barlow et al., 2008]. PDSCs display multi-lineage differentiation potential, and they are free of ethical concerns, easily accessible, abundant, and strongly immunosuppressive [Huttmann et al., 2003; In 't Anker et al., 2004; Chang et al., 2006]. Parolini et al. [2008] described the minimal criteria for defining PDSCs: (i) fetal origin; (ii) generation of fibroblast colony-forming units; (iii) specific patterns of surface antigen expression; and (iv) potential to differentiate into one or more lineages. PDSCs isolated from the placentas of normal-term human infants include amniotic epithelial cells (AECs), amniotic mesenchymal stromal cells (AMSCs), chorionic mesenchymal stromal cells (CMSCs), umbilical mesenchymal stromal cells (UMSCs) from Wharton's jelly, and trophoblast stem cells [Parolini et al., 2008; Tsai et al., 2009]. Moreover, PDSCs have the potential to differentiate in vitro into hepatocyte-like cells and insulin-positive cells, as well as mesodermal lineages [Bailo et al., 2004; Chang et al., 2007; Parolini et al., 2008].

Recently, the transplantation of PDSCs into mice with bleomycin-induced lung fibrosis significantly reduced the severity of lung fibrosis and neutrophil infiltration [Cargnoni et al., 2009]. However, the therapeutic potential of chorionic plate-derived mesenchymal stem cells (CP-MSCs) isolated from the placenta has not been evaluated using in vivo models of liver disease.

The present study was conducted to characterize CP-MSCs isolated from the placentas of normal-term infants, to test the potential of CP-MSCs to differentiate into functional hepatocyte-like cells, and to evaluate the therapeutic potential of CP-MSCs by measuring their effects on the structural and functional regeneration of the liver in CCl_4-injured rats.

MATERIALS AND METHODS

ISOLATION AND CULTIVATION OF CP-MSCS FROM PLACENTA

CP-MSCs were isolated from normal placentas. Placentas were considered normal when the pregnancy was free of medical, obstetrical, and surgical complications and delivery occurred at term (gestation $\geq$37 weeks). All of the women who contributed to this study provided written informed consent prior to sample collection. The isolation of samples and their subsequent utilization for research purposes were approved by the Institutional Review Board of CHA General Hospital, Seoul, Korea. CP-MSCs were harvested from the chorionic plate of placentas obtained following Cesarean section. Briefly, the chorioamniotic membrane was peeled and separated from the placenta. Then, the amnion and the innermost membrane from the chorion and decidua were removed. Cells scraped from the membrane were treated with 0.5% collagenase IV (Sigma–Aldrich, St. Louis, MO) for 30 min at 37°C. The harvested cells were cultured at 2×10^5 cells/mm^3 in T25 flasks (BD Biosciences, San Jose, CA) in Ham's F-12/DMEM supplemented with 10% fetal bovine serum (FBS) and 1% penicillin/streptomycin (P/S; all from GIBCO, New York, NY).

CO-CULTURE OF CP-MSCS WITH RAT HEPATIC STELLATE CELLS EXPOSED TO TGF-β

Rat T-HSC/Cl-6 hepatic stellate cells were seeded at 2×10^4 cells/insert in six-well plates, and CP-MSCs were added to the corresponding Transwell cell culture inserts (5-μM pore PET membrane; BD Biosciences). The cells were co-cultured in Ham's F-12/DMEM containing TGF-β (2 ng/ml) for 24 and 48 h. The cells were harvested, and the expression of type I collagen (Col I) was analyzed by RT-PCR. Supernatant matrix metalloproteinase (MMP) activity was measured by zymography.

RNA ISOLATION AND RT-PCR ANALYSIS

CP-MSCs and rat liver tissue were homogenized and lysed, and total RNA was prepared using TRIzol reagent (Invitrogen, Carlsbad, CA). Total RNA samples (2 μg) were reverse transcribed using SuperScript™ III reverse transcriptase (Invitrogen). The resulting cDNA was amplified by PCR using the primers listed in Table I and the following thermal conditions: 5 min at 95°C, followed by 24–31 cycles of 94°C for 30 s, 48–60°C for 1 min, and 72°C for 1 min. PCR products were visualized and photographed after electrophoresis in 2% (w/v) agarose gels containing 0.5 μg/ml ethidium bromide (Promega, Madison, WI).

FACS ANALYSIS

Cells were dissociated in cell dissociation buffer (GIBCO) and incubated for 20 min with antigen-specific antibody (BD Bioscience) or isotype control, followed by incubation for 30 min with various fluorescence-conjugated anti-human IgG antibodies (diluted 1: 200; Vector Laboratories, Burlingame, CA). Propidium iodide (PI) (5 ng/ml; Sigma–Aldrich) was used to identify non-viable cells. FACS analysis was performed using a FACSVantage flow cytometer (BD Biosciences).

IN VITRO DIFFERENTIATION OF CP-MSCS TO MESODERMAL LINEAGES

To analyze the potential of CP-MSCs to differentiate into mesodermal lineages, we used passage-five CP-MSCs plated at a density of 5×10^3 cells/cm^2. To induce osteogenic differentiation, CP-MSCs were cultured in osteogenic induction medium containing

TABLE I. Sequence of Primers Used for RT-PCR and Length of Fragments

Genes	Sequence	T_m (°C)	Size (bp)
Oct4	F: 5′-ACA CTC GGA CCA CGT CTT TC-3′		
	R: 5′-CGT TCT CTT TGG AAA GGT GTT C-3′	54	300
Nanog	F: 5′-TTC TTG ACT GGG ACC TTG TC-3′		
	R: 5′-GCT TGC CTT GCT TTG AAG CA-3′	54	300
Sox2	F: 5′-GGG CAG CGT GTA CTT ATC CT-3′		
	R: 5′-AGA ACC CCA AGA TGC ACA AC-3′	52	200
NF-68	F: 5′-GAG TGA AAT GGC ACG ATA CCT A-3′		
	R: 5′-TTT CCT CTC CTT CTT CTT CAC CTT C-3′	58	500
Cardiac	F: 5′-GGA GTT ATG GTG GGT ATG GGT C-3′		
	R: 5′-AGT GGT GAC AAA GGA GTA GCC A-3′	58	500
AFP	F: 5′-AGC TTG GTG GAT GAA AC-3′		
	R: 5′-TCC AAC AGG CCT GAG AAA TC-3′	50	200
HLA-G	F: 5′-GCG GCT ACT ACA ACC AGA GC-3′		
	R: 5′-GCA CAT GGC ACG TGT ATC TC-3′	58	900
TERT	F: 5′-GAG CTG ACG TGG AAG ATG AG-3′		
	R: 5′-CTT CAA GTG CTG TCT GAT TCC AAT G-3′	55	300
β-actin	F: 5′-TCC TTC TGC ATC CTG TCA GCA-3′		
	R: 5′-CAG GAG ATG GCC ACT GCC GCA-3′	58	300
CK18	F: 5′-GAG ATC GAG GCT CTC AAG GA-3′		
	R: 5′-CAA GCT GGC CTT CAG ATT TC-3′	55	400
CK19	F: 5′-GGG TCT TGA GAT TGA GCT GCA GT-3′		
	R: 5′-CCA GAA GAC ACC CTC CAA AGG AC-3′	60	342
HNF1α	F: 5′-TAC ACC ACT CTG GCA GCC ACA CT-3′		
	R: 5′-CGG TGG GTA CAT TGG TGA CAG AAC-3′	58	114
HNF1β	F: 5′-GCA GAA CTC ACA CAT GTA CGC-3′		
	R: 5′-AGG AGT CCT TGA CAT CGT GG-3′	60	396
HNF4α	F: 5′-CTG CTC GGA GCC ACC AAG AGA TCCATG-3′		
	R: 5′-ATC ATC TGC CAC GTG ATG CTC TGCA-3′	55	370
CXCR4	F: 5′-ACG TCA GTG AGG CAG ATG-3′		
	R: 5′-GAT GAC TGT GGT CTT GAG-3′	58	202
Albumin	F: 5′-CCC CAA GTG TCA ACT CCA AC-3′		
	R: 5′-CTC CTT ATC GTC AGC CTT GC-3′	54	450
TAT	F: 5′-AAC GAT GTG GAG TTC ACG G-3′		
	R: 5′-GAC ACA TCC TCA GGA GAA TGG-3′	59	288
TTR	F: 5′-AAC CAG TGA GTC TGG AGA GC-3′		
	R: 5′-TGC CTG GAC TTC TAA CAT AGC-3′	58	258
α-SMA	F: 5′-ACT GGG ACG ACA TGG AAA AG-3′		
	R: 5′-CAT CTC CAG AGT CCA GCA CA-3′	54	240
Col I	F: 5′-CAT CTC AGA AGC AGA ATC TCC-3′		
	R: 5′-CCA TAA ACC ACA CTA TCA CCT C-3′	59	360
28s rRNA	F: 5′-TTG AAA ATC CGG GGG AGA G-3′		
	R: 5′-ACA TTG TTC CAA CAT GCC AG-3′	52	100

1 μM dexamethasone, 10 mM glycerol 2-phosphate, 50 μM L-ascorbic acid 2-phosphate (all from Sigma–Aldrich), 10% FBS, and 1% P/S. The growth medium was replaced twice weekly. Following the induction of osteogenic differentiation, the cells were fixed in 4% formaldehyde and subjected to von Kossa staining by incubation with a 2% silver nitrate solution (Sigma–Aldrich) and simultaneous exposure to a 60-W lamp. To induce adipogenic differentiation, CP-MSCs were cultured in adipogenic induction medium containing 1 μM dexamethasone, 0.5 mM isobutyl methylxanthine, 0.2 mM indomethacin, 1.7 μM insulin, 10% FBS, and 1% P/S. The growth medium was replaced twice weekly. After 21 days, the cells were fixed in 4% formaldehyde, and lipid vesicles were visualized by staining with Oil Red O for 1 h and counterstaining with Mayer's hematoxylin (both from Sigma–Aldrich) for 1 min. To induce chondrogenic differentiation, 5×10^5 CP-MSCs were collected as a pellet by centrifugation at 1,000 rpm for 5 min and then cultured in chondrogenic medium containing 100 nM dexamethasone, 100 mM sodium pyruvate, 50 μM L-ascorbic acid 2-phosphate (all from Sigma–Aldrich), 1× insulin-transferrin-selenium (ITS^+) premix (GIBCO), TGF-β1 (Peprotech EC, Ltd., London, England), and 1% P/S. After 21 days, the cell pellets were fixed in 4% formaldehyde, the cryomolded pellets were sectioned to a thickness of 10 μm, and the sections were stained with Alcian blue (Sigma–Aldrich).

IN VITRO DIFFERENTIATION OF CP-MSCS TO HEPATOCYTES

Hepatic differentiation of CP-MSCs was performed as described previously [Talens-Visconti et al., 2007] with modifications. Prior to hepatic differentiation, passage-five cells were plated at a density of 2×10^4 cells/cm^2 in basal medium (60% DMEM-LG, 40% MCDB201, 2% FBS, and 1% P/S) containing 20 ng/ml EGF and 10 ng/ml bFGF. Cells were grown to 60% confluence and then incubated for 7 days in basal medium supplemented with 2% FBS, 20 ng/ml HGF, 10 ng/ml bFGF, and 0.61 g/L nicotinamide. To induce maturation, the cells were treated with maturation medium (basal medium supplemented with 2% FBS, 1 μM dexamethasone, 50 mg/ml ITS^+ premix, and 20 ng/ml oncostatin M) for a further 2 weeks. The medium was replaced every 3 days. Hepatogenic differentiation was assessed by RT-PCR analysis of liver-specific genes.

INDUCTION OF LIVER INJURY USING CCL_4 AND TRANSPLANTATION OF CP-MSCS INTO CCL_4-INJURED RATS

We conducted all animal experiments using approved protocols and according to the National Institutes of Health guidelines. To induce liver injury in our experimental animals, we used a previously described protocol [Constandinou et al., 2005] with modifications. Six-week-old male Sprague–Dawley rats (n = 6) received intraperitoneal injections of CCl_4 (Sigma–Aldrich) dissolved at 0.8 mg/ml in

corn oil. CCl_4 was administered at 0.2 ml/100 g body weight (approximately 1.6 g/kg) twice a week for 9 weeks. An equal volume of corn oil was administered to control animals. In order to trace the transplanted CP-MSCs in CCl_4-injured rats, CP-MSCs were labeled using a PKH26 Red Fluorescent Cell Linker kit (Sigma–Aldrich) according to the manufacturer's instructions. The PKH26-labeled CP-MSCs (2×10^6) were directly transplanted into the right liver lobe of each CCl_4-injured rat by injection at a depth of 5 mm. Blood and liver tissues were collected 1, 2, and 3 weeks post-transplantation. The presence of grafted CP-MSCs in the livers of CCl_4-injured rats was assessed by histopathological examination.

BLOOD CHEMISTRY ANALYSIS

The levels of glutamate–oxaloacetate transaminase/aspartate transaminase (GOT/AST), glutamate–pyruvate transaminase/alanine transaminase (GPT/ALT), total bilirubin (TBIL), and albumin in the blood collected from the animals at 1, 2, and 3 weeks post-transplantation were measured using a Dry-Chem 3500i Auto Biochemistry Detector (Fujifilm).

HISTOPATHOLOGICAL ANALYSIS

Liver tissue was fixed in 10% (v/v) buffered formaldehyde, embedded in paraffin, and sectioned to a thickness of 5 μm. Tissue sections were stained with hematoxylin and eosin (H&E). Masson's trichrome staining (MT) and periodic acid shift (PAS) staining were performed to examine liver collagen deposition and glycogen storage, respectively. Liver fibrosis in CCl_4-injured rats was scored according to the histopathological criteria of Nanji et al. [1989] with modifications: 0, no fibrosis; 1, fibrosis confined to enlarged portal zones; 2, periportal or portal-portal septa with intact architecture; 3, distorted architecture (septal fibrosis, bridging) without obvious cirrhosis; and 4, probable or definite cirrhosis.

IMMUNOSTAINING

To trace the transplanted human CP-MSCs, the remaining specimens were embedded in Tissue-Tek O.C.T. compound (Sakura Finetek, CA), frozen, and sectioned at 8-μm thickness. The tissue sections were stained with specific anti-human cytokeratin 18 (CK18; Sigma–Aldrich), anti-human cytokeratin 19 (CK19; Sigma-Aldrich), and anti-human hepatocyte antibodies (DAKO, Carpinteria, CA). Primary antibody binding was visualized using FITC-conjugated anti-mouse or cyanine-conjugated anti-goat secondary IgGs (Molecular Probes; Invitrogen). Images were acquired using a LSM 510 META confocal microscope (Carl Zeiss, Inc., Thornwood, NY). Human nucleolin in transplanted CP-MSCs was immunostained using a Vectastain ABC system and diaminobenzidine (DAB) substrate (both from Vector Laboratories) according to the manufacturer's instructions, with minor modifications. Mouse anti-human nucleolin antibody (1:100; Chemicon, Rosemont, IL) was used as the primary antibody, with a biotinylated secondary antibody, horseradish peroxidase conjugated streptavidin–biotin complex, and DAB to generate a chromatic signal. Antigens were retrieved by microwaving for 7 min in 10 mM citrate buffer, pH 6.0.

WESTERN BLOT ANALYSIS

To quantify liver levels of Col I, α-SMA, MMP-9, and albumin, liver tissue was homogenized in protein extraction solution (Intron, Seongnam-Si, Korea). The homogenates were sonicated for 20 s and centrifuged. The supernatants were analyzed by Western blotting. Briefly, protein lysates (50 μg) were incubated at 95°C for 3 min, subjected to 12% sodium dodecyl sulfate (SDS)–polyacrylamide gel electrophoresis (PAGE), and electrophoretically transferred to PVDF membranes (90 V for 80 min). After incubation in blocking buffer for 1 h at room temperature, the membranes were incubated with anti-Col I monoclonal antibody (diluted 1:5,000; Abcam, Cambridge, UK), anti-α-SMA monoclonal antibody (1:5,000; Abcam), anti-MMP-9 polyclonal antibody (1:1500; R&D Systems, Minneapolis, MN), anti-albumin monoclonal antibody (1:3,000; Sigma–Aldrich), or anti-β-actin monoclonal antibody (1:1,000; Santa Cruz, CA) at 4°C overnight, followed by incubation with horseradish peroxidase-conjugated anti-mouse or anti-goat secondary antibody (diluted 1:3,000; Vector Laboratories). Protein bands were visualized using an ECL Advance Western Blotting Detection System (Amersham, Uppsala, Sweden).

ZYMOGRAPHY

Culture supernatants from co-cultured T-HSC/Cl-6 cells and CP-MSCs (70 μl per sample) were analyzed by SDS–PAGE zymography in gels impregnated with 0.5% gelatin (Sigma–Aldrich). Following electrophoresis, the gels were incubated overnight at 37°C in a buffer containing 50 mM Tris–HCl (pH 7.4), 0.2 M NaCl, 5 mM $CaCl_2$, and 1% Triton X-100. Enzymatic activity was detected by staining with 0.1% Coomassie Blue in 30% methanol/10% acetic acid.

INDOCYANINE GREEN (ICG) UPTAKE AND EXCRETION ASSAYS

To analyze ICG uptake, differentiated CP-MSCs were incubated in ICG solution (1 mg/ml; Dongindang Pharm. Co., Korea) at 37°C for 90 min and then rinsed with PBS. The culture medium was replaced, and the uptake of ICG by CP-MSCs was measured using an inverted microscope. To evaluate hepatic function, hepatic excretion of ICG was measured in vivo. ICG dissolved in sterile water (0.5 mg/ml) was administered to each rat via the tail vein [Yamada et al., 2002]. Blood samples were removed via the ventricular artery 15 min later, and absorbance at 805 nm was measured using a spectrophotometer.

UREA PRODUCTION AND MMP-9 ELISA

Undifferentiated and differentiated CP-MSCs were cultured for 24 h in supplemented medium. Supernatants were collected, and urea production was determined using a colorimetric Quantichrom urea assay kit (Bioassay Systems, Hayward, CA). To quantify MMP-9 levels in T-HSC/Cl-6 cells exposed to TGF-β (2 ng/ml) and co-cultured with CP-MSCs, culture supernatants were analyzed using a human MMP9 ELISA kit (RayBiotech Inc., Norcross GA). Fresh culture medium and HepG2 cells were used as negative and positive controls, respectively.

STATISTICAL ANALYSIS

All experiments were performed in duplicate and were repeated at least three times. PCR data were quantified densitometrically. Data

were analyzed by one-way or two-way ANOVA. The following dependent variables were analyzed by two-way ANOVA: the Col I/28s rRNA ratio (collagen synthesis analyses) and GOT/AST, GPT/ALT, TBIL, and albumin levels (blood analyses). Data are presented as means ± SD. A *P*-value <0.05 was considered to indicate statistical significance.

RESULTS

CP-MSC morphology was similar to that of traditional MSCs (Fig. 1A), and a specific marker of embryonic stem cells (Oct-4) was detected in the CP-MSCs (Fig. 1B). In addition, three stem cell markers (Nanog, Sox2, and TERT), three germ layer markers [NF68, cardiac muscle, and α-fetoprotein (AFP)], and an immunomodulator gene (HLA-G) were all expressed in the CP-MSCs. These results suggest that the CP-MSCs have the potential for self-renewal and the capacity to differentiate into multiple lineages.

To confirm the surface phenotypes of the CP-MSCs, we performed FACS analysis using various mouse anti-human antibodies (Fig. 1C). The phenotypes of the CP-MSCs were similar to those of BM-MSCs, that is, negative for hematopoietic markers such as CD31, CD33, CD34, CD45, CD51/61, and HLA-DR; and positive for non-hematopoietic markers, including CD13, CD44, CD90, CD105, and HLA-ABC. There were no differences in the expression levels of any of these markers between the CP-MSCs and BM-MSCs. Furthermore, the surface expression of CD56, CD71, CD95, and HLA-G was detected in the CP-MSCs.

To test the potential of CP-MSCs to differentiate into mesodermal lineages, we induced osteogenic, adipogenic, and chondrogenic differentiation of the CP-MSCs. As shown in Figure 1D, the levels of dense mineralized phosphate deposits (assessed by von Kossa staining) were increased following osteogenic differentiation of the CP-MSCs. Lipid droplet accumulation in the CP-MSCs following adipogenic differentiation was detected by Oil Red O staining. The chondrogenic differentiation of the CP-MSCs was verified by

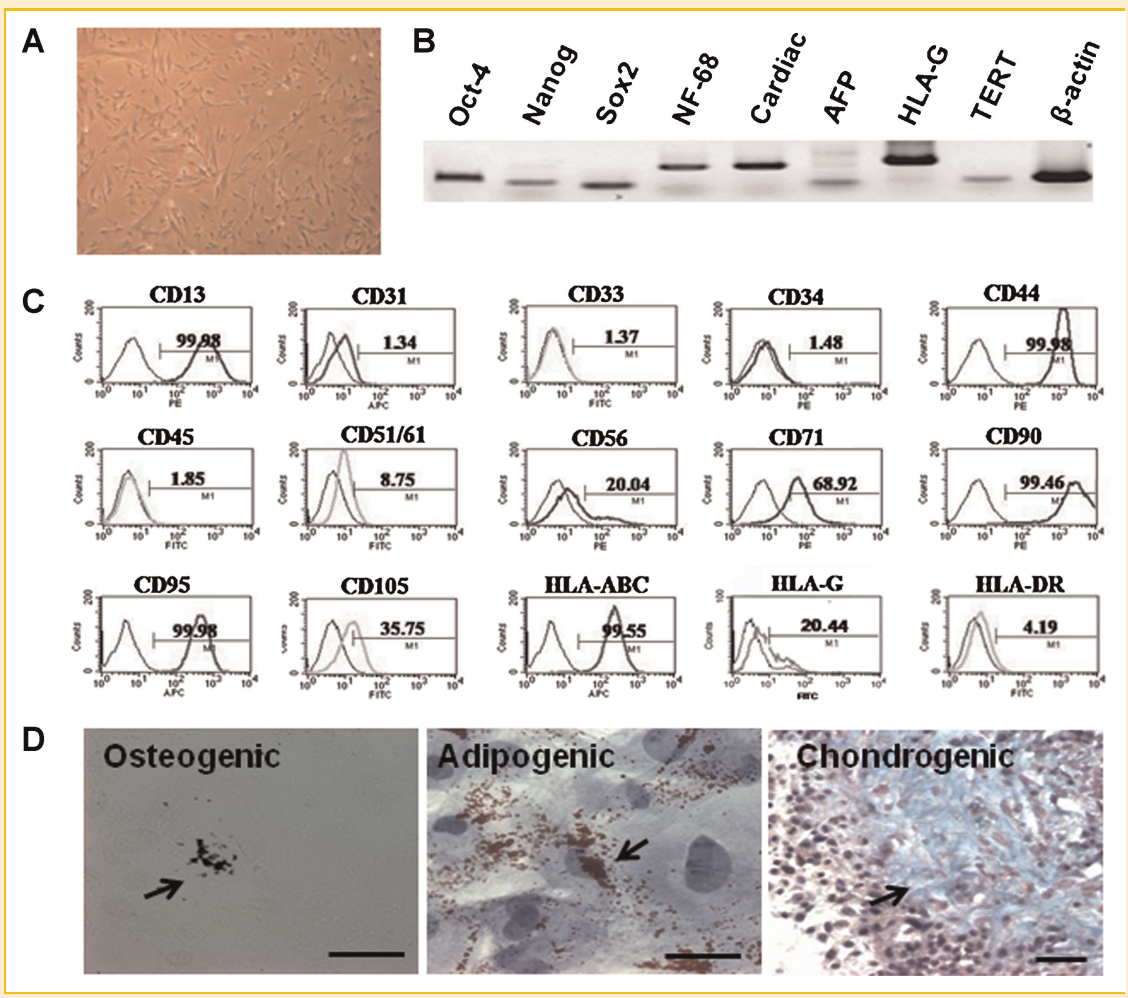

Fig. 1. Characterization of CP-MSCs. CP-MSCs were assessed at passage numbers 8 through 10. A: The morphology of CP-MSCs was similar to the round-spindle shape of mesenchymal stem cells (×100). B: RT-PCR analysis for stem cell markers in CP-MSCs. C: FACS analysis of the expression of surface markers in CP-MSCs. The percentages are indicated along with the fluorescence intensities. D: Differentiation of CP-MSCs. Osteogenic, adipogenic, and chondrogenic differentiation was confirmed by von Kossa, Oil Red O, and Alcian blue staining, respectively. Scale bars: 100 μm. [Color figure can be viewed in the online issue, which is available at wileyonlinelibrary.com.]

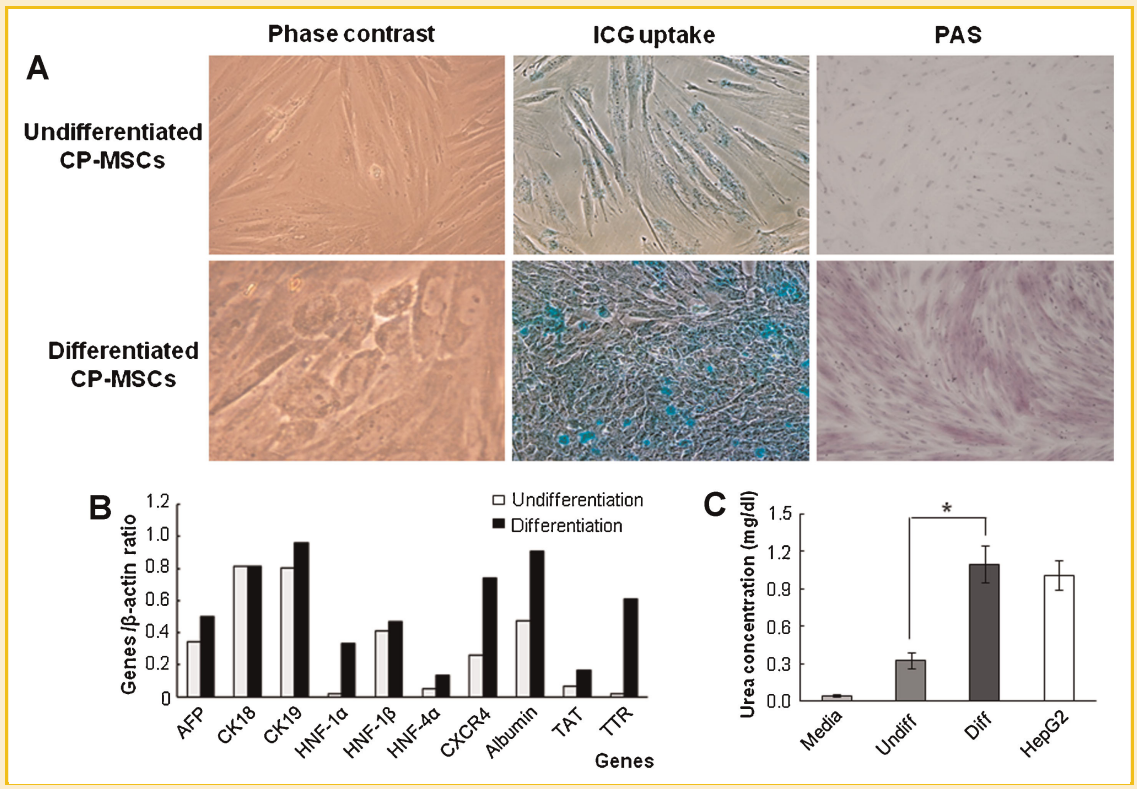

Fig. 2. Hepatogenic differentiation of CP-MSCs. A: The morphological changes (Left), ICG uptake (Middle), and glycogen storage using PAS staining (Right) of CP-MSCs between undifferentiation (Upper) and differentiation (Lower), following hepatogenic differentiation (200×). B: Expression of various hepatogenic-specific genes during hepatogenic differentiation by RT-PCR analysis. C: Urea production in CP-MSCs. Urea production in CP-MSCs differentiated into hepatocyte-like cells was increased threefold compared to that in undifferentiated CP-MSCs ($P < 0.005$). Undiff means undifferentiated CP-MSCs; Diff means hepatic differentiated CP-MSCs. HepG2 used as a positive control of urea production. [Color figure can be viewed in the online issue, which is available at wileyonlinelibrary.com.]

Alcian blue staining. Collectively, these results suggest that the CP-MSCs have the potential to differentiate into several mesodermal lineages, including osteogenic, adipogenic, and chondrogenic lineages.

During hepatogenic differentiation, the CP-MSCs gradually exhibited a change in morphology, from a spindle shape to a characteristic polygonal hepatocyte-like morphology, and began to cluster (Fig. 2A, left). Although the CP-MSCs did not take up ICG before differentiation, they took up large amounts of ICG following hepatogenic differentiation (Fig. 2A, middle) and exhibited glycogen storage (Fig. 2A, right). The switching on and off of several genes was involved in hepatic function plays a critical role in the progression of hepatogenesis during early embryogenesis [Costa and Grayson, 1991; Hay et al., 2008]. Gene expression analysis showed that patterns of gene expression during differentiation of the CP-MSCs mirrored those observed during hepatogenesis. The expression of the hepatocyte-specific transcription factors human nuclear factor (HNF)-1α and -4α was increased in the CP-MSCs during hepatogenic differentiation, as was the expression of hepatoblast markers such as AFP and CK19, and transthyretin, which is controlled by HNF-4α. In addition, the expression levels of CXCR4, TAT, and albumin were higher in differentiated CP-MSCs compared with undifferentiated cells (Fig. 2B). Furthermore, urea production was significantly higher in differentiated CP-MSCs than in undifferentiated cells ($P < 0.005$; Fig. 2C). These results confirm the effective induction of hepatogenic differentiation and suggest that the CP-MSCs can differentiate into functional hepatocyte-like cells as well as hepatoblasts and mature hepatocytes.

To evaluate the function of CP-MSCs in an in vivo model of severe liver injury, we induced liver injury in rats through repeated administration of a high concentration of CCl_4 (approximately 1.6 g/kg, twice a week) over the course of 9 weeks (Fig. 3A). We confirmed the suitability of CCl_4-induced liver failure as a model of early cirrhosis by blood chemistry (Table II) and pathological analyses. Compared with the livers of control animals, the livers of CCl_4-injured rats displayed a range of severe injury, including bridging fibrosis connecting neighboring portal veins and central veins, various lipid changes, and increased inflammation (Fig. 3B).

The fate of transplanted PKH26-labeled CP-MSCs was observed in the livers of recipient animals by fluorescence microscopy (Fig. 4A, left) and immunohistochemistry using an antibody specific for human nucleolin (Fig. 4A, right). Immunofluorescence analysis revealed the expression of the human hepatocyte markers CK18 and CK19 in transplanted CP-MSCs in the injured rat livers (Fig. 4B). These results demonstrate that the CP-MSCs were engrafted successfully and that some CP-MSCs differentiated into hepatocytes following transplantation into CCl_4-treated rats. This latter process may facilitate liver regeneration.

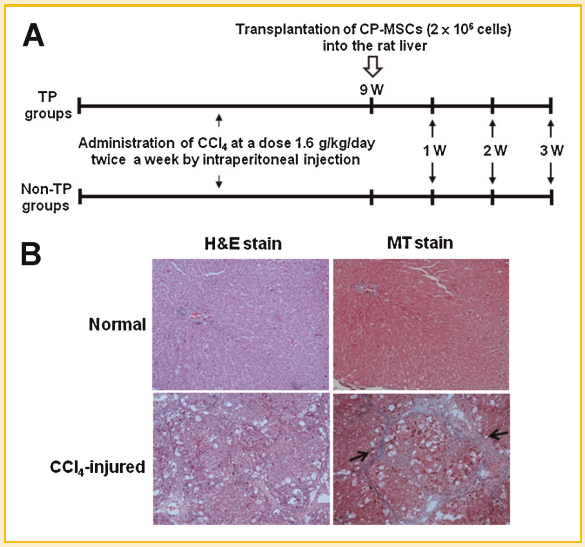

Fig. 3. Generation of the CCl_4-injured rat liver disease model. A: Diagram of experimental scheme. B: Histopathological analysis of the normal rat liver (Upper) and the CCl_4-injured rat liver disease model (Lower) using H&E (Left) and MT (Right) staining (100×). Arrows indicate formation of collagen bridging fibrosis. TP: transplantation; W: week. [Color figure can be viewed in the online issue, which is available at wileyonlinelibrary.com.]

To determine whether CP-MSCs can induce regeneration of damaged liver tissues, we analyzed the expression of Col I, α-SMA, and albumin, which are markers of liver damage, in the livers of transplanted (TP) and non-transplanted rats (Non-TP). The expression of both Col I and α-SMA was dramatically increased in CCl_4-injured livers compared with controls, and the expression of albumin was decreased (Fig. 5). Col I mRNA expression was significantly lower in TP rats than in Non-TP animals until 3 weeks post-transplantation ($P < 0.05$; Fig. 5A), the mRNA expression level of α-SMA was significantly lower until 2 weeks post-transplantation ($P < 0.05$; Fig. 5B), and albumin mRNA expression was significantly higher in TP rats than in Non-TP animals at 1 and 2 weeks post-transplantation ($P < 0.05$ and $P < 0.005$, respectively; Fig. 5C). Based on Western blot analysis, Col I and α-SMA protein expression was markedly lower in TP rats than in Non-TP rats until 2 weeks post-transplantation, and albumin protein expression was higher in TP rats until 3 weeks post-transplantation (Fig. 5D). These data are in agreement with the findings of mRNA expression. In addition, the expression of MMP-9 protein, which inhibits collagen synthesis and deposition, was elevated until 2 weeks post-transplantation in TP rats (Fig. 5D).

Histological analysis of the rat liver tissues showed greater changes in lipid accumulation and stronger macrophage infiltration in non-TP rats than in TP rats. Collagen deposition was dramatically lower in TP rats than in Non-TP animals (Fig. 6A). TP rats also displayed an overall reduction and amelioration of bridging fibrosis connecting neighboring portal and central veins. Furthermore, liver damage scores assigned according to four-tiered cirrhosis criteria were lower in TP rats (Table IV). These findings were consistent with the results of the RT-PCR and Western blot analyses.

TABLE II. An Animal Model of Liver Failure

	GOT/AST	GPT/ALT	TBIL	Albumin
Control	112.5 ± 6.5	46.5 ± 5.3	0.63 ± 0.07	3.42 ± 0.05
CCl_4 (9W)	925.4 ± 34[a]	685 ± 74[a]	1.18 ± 0.2[a]	3.28 ± 0.040[a]

[a]*P*-values were compared with control group ($P < 0.05$).

To test whether the engrafted CP-MSCs improved hepatic function, we measured ICG uptake and excretion. Changes in ICG excretion indicate pathophysiological alterations in liver function. Normally, about 90% of the ICG taken up into the liver is released into the blood within 15 min [Yamada et al., 2002]. Compared with control rats, the CCl_4-injured rats showed significantly lower ICG release ($P < 0.005$; Fig. 6B). However, the TP rats exhibited significantly higher ICG release the non-TP rats during all 3 weeks of the study ($P < 0.005$). ICG release gradually increased in TP rats, reaching levels comparable to control levels by 3 weeks post-transplantation ($P > 0.16$). In contrast, ICG release in Non-TP rats did not increase after 2 weeks (Fig. 6B). Moreover, in blood chemistry analyses, the levels of GOT, GPT, and TBIL were significantly lower in TP rats than in non-TP rats (Table III). These findings indicate that engrafted CP-MSCs greatly improved hepatic function in the CCl_4-injured liver.

Based on our observation of decreased collagen deposition and increased MMP-9 expression in TP rats compared with non-TP animals (Fig. 5), we hypothesized that MMPs secreted from transplanted CP-MSCs may contribute to the recovery of liver function by decreasing collagen deposition. Exposing hepatic stellate cells to a sustained low dose of TGF-β has been shown to stimulate Col I synthesis by inducing the transcription factor Snail1 and activating Smad2/3 signaling [Kaimori et al., 2007]. Therefore, we investigated whether co-culture with CP-MSCs influenced collagen synthesis in T-HSC/Cl-6 hepatic stellate cells exposed to TGF-β. Col I mRNA expression gradually increased in the T-HSC/Cl-6 cells cultured alone in medium containing TGF-β (2 ng/ml). In contrast, Col I expression decreased dramatically in T-HSC/Cl-6 cells co-cultured with CP-MSCs in the presence of TGF-β (Fig. 7A). We also performed zymographic analyses to measured MMP activity in the co-cultures. Exposure to TGF-β for 24 h reduced MMP-2 and MMP-9 activities in T-HSC/Cl-6 cells, and both activities increased slightly following treatment with TGF-β for a further 24 h. In the co-cultures, MMP-2 and MMP-9 activities were detected and increased in a time-dependent manner (Fig. 7B). An ELISA confirmed that MMP-9 expression was higher in T-HSC/Cl-6 cells co-cultured with CP-MSCs compared with T-HSC/Cl-6 cells cultured alone (Fig. 7C, $P < 0.05$). These findings suggest that CP-MSCs may improve hepatic function in CCl_4-injured rats by increasing MMP-2 and MMP-9 activities, thereby limiting the synthesis and deposition of Col I.

DISCUSSION

In the present study, we demonstrated for the first time that the transplantation of CP-MSCs derived from the chorionic plate of the placenta may be a feasible treatment for the CCl_4-injured liver. CP-MSCs were transplanted into rats with severely injured livers, and

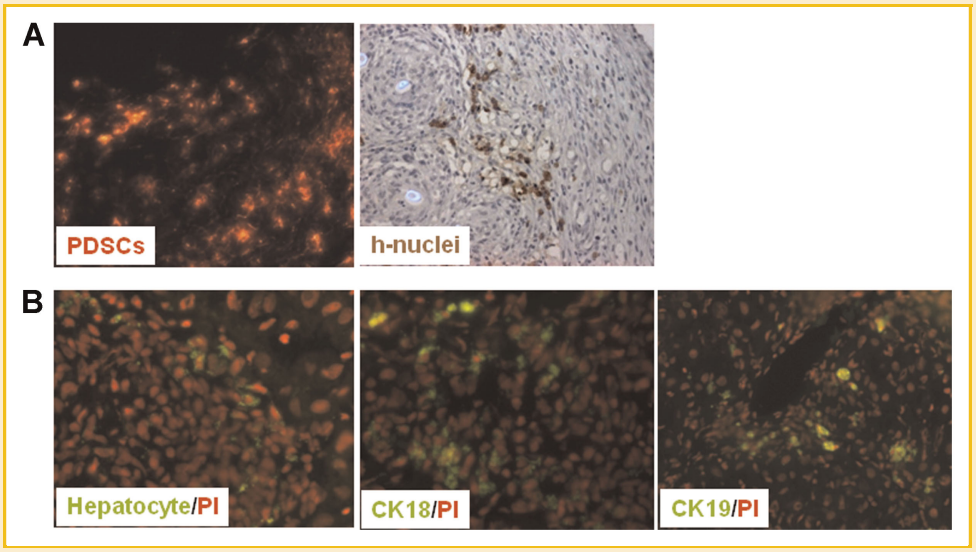

Fig. 4. Engraftment of CP-MSCs into the CCl_4-injured rat liver disease model. A: PKH-labeled CP-MSCs engrafted into CCl_4-injured rat liver tissues (Left); analysis of CP-MSCs engrafted into CCl_4-injured rat liver tissues using immunohistochemistry of human-specific nuclei (Right). B: Expression of hepatocyte-related markers including human hepatocyte (Left), CK18 (Middle), and CK19 (Right) using immunofluorescence. PI was used as a nuclear stain (100×). [Color figure can be viewed in the online issue, which is available at wileyonlinelibrary.com.]

the anti-fibrotic effects of the CP-MSCs were evaluated in vitro and in vivo.

Transplantation of adult stem cells has previously been used to treat various degenerative diseases [Daley and Scadden, 2008]. However, the clinical feasibility of this approach remains controversial because of the differences between humans and model animals. In animal models, CCl_4 is widely used experimentally to elicit liver damage; however, it decomposes in the lipids of damaged cells and leads to rapid breakdown of the endoplasmic reticulum and loss of its function. CCl_4-induced liver injury is both

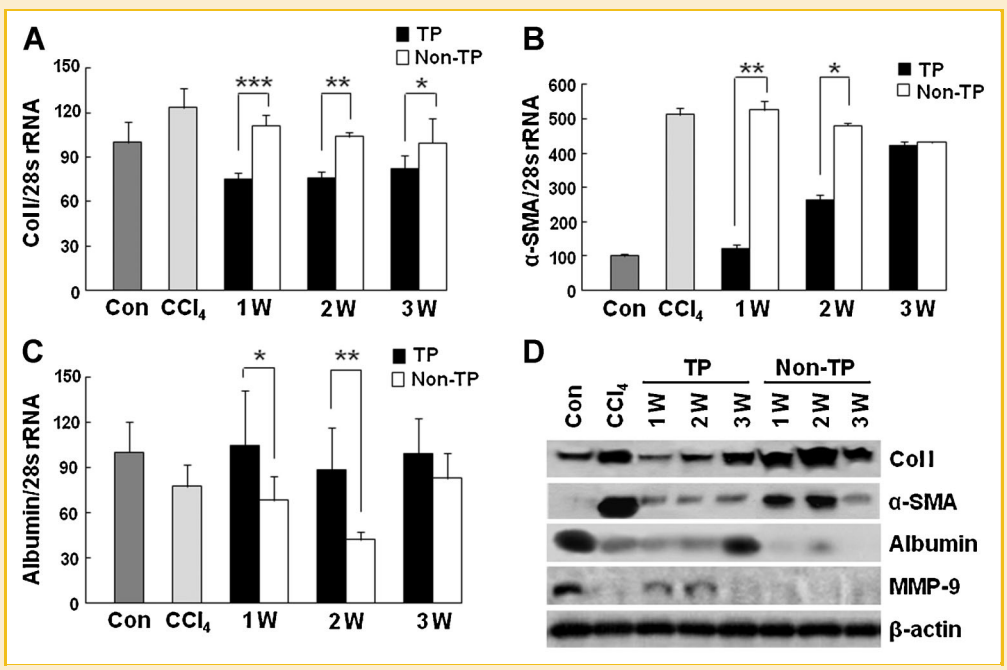

Fig. 5. Liver damage-related gene expression following the transplantation of CP-MSCs into CCl_4-injured rat livers. The degree of liver fibrosis was measured semiquantitatively via the mRNA expression of Col I (A), α-SMA (B), and albumin (C) by RT-PCR. Data are expressed as the mean ± SD from five mice for each group. The asterisk indicates a significant difference between the groups. D: Expression of Col I, α-SMA, albumin, and MMP-9 in between the TP group and the non-TP group using Western blot. β-actin was used as loading control. * indicates $P < 0.05$, ** indicates $P < 0.005$ and *** indicates $P < 0.001$ compared with Non-TP group. TP: transplantation, W: week.

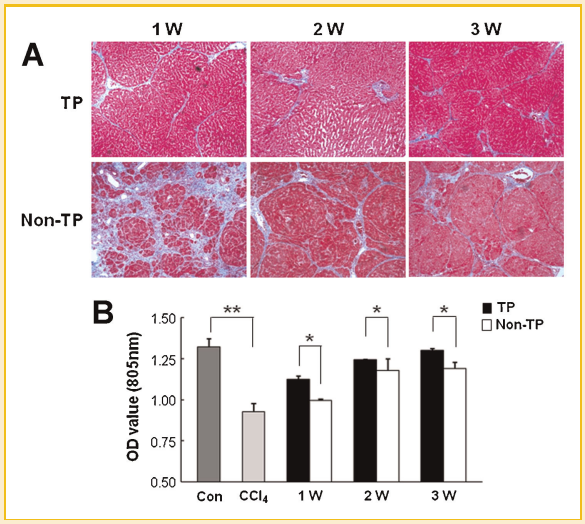

Fig. 6. Therapeutic effects of the transplantation of CP-MSCs into the CCl_4-injured rat liver. Liver tissues were obtained from TP group (Upper) and Non-TP group (Lower) at 1, 2, and 3 weeks after generation of the CCl_4-injured rat liver disease model for 9 weeks. A: After CP-MSCs transplantation into liver tissues, the degree of liver fibrosis was analyzed from 1–3 weeks using MT staining(100×). B: After CP-MSCs transplantation into liver tissues, the degree of liver function was analyzed by ICG uptake and excretion assays. Data are expressed as the mean ± SD from five mice for each group. * indicates $P < 0.005$ and ** indicates $P < 0.001$. [Color figure can be viewed in the online issue, which is available at wileyonlinelibrary.com.]

severe and extremely rapid in its onset, and it ultimately manifests histologically as hepatic steatosis, fibrosis, hepatocellular death, and carcinogenicity, Nevertheless, damaged hepatocytes regenerate easily in the absence of further exposure to CCl_4 [Iredale, 2007]. Animal injuries caused by low-dose and short-term injection of CCl_4 show rapid hepatocyte regeneration on a time scale dependent on the species used, making it necessary to confirm liver damage comparable with cirrhosis in any CCl_4-injured liver model [Constandinou et al., 2005; Lee et al., 2005]. Therefore, after generating a rat model of severe liver injury through high-dose (1.6 g/kg), long-term (9 weeks) treatment with CCl_4, we confirmed the injury by blood chemistry and histopathological assays (Table II, Fig. 3B) and tested liver function by ICG assay (Fig. 6B). Our data showed that the damaged livers did not exhibit full hepatocyte regeneration after a 3-week recovery period (Table IV). It should be noted that the spontaneous recovery of damaged hepatocytes and liver tissues has been unduly ignored in animal models described by other researchers.

TABLE III. Blood Chemistry Analysis

Weeks	Groups	GOT/AST	GPT/ALT	TBIL	Albumin
1W	Non-TP	158.6 ± 24.6	56.6 ± 14.4	0.5 ± 0.1	3.5 ± 0.1
	TP	121.4 ± 31.2[a]	38.6 ± 14.4[a]	0.4 ± 0.1	2.7 ± 0.1[a]
2W	Non-TP	191.6 ± 27.9	90.0 ± 14.4	0.9 ± 0.1	3.0 ± 0.1
	TP	21.1 ± 31.2[a]	49.6 ± 16.1[a]	0.4 ± 0.1[a]	2.6 ± 0.2[a]
3W	Non-TP	191.4 ± 23.6	69.0 ± 12.2	0.4 ± 0.1	3.3 ± 0.1
	TP	53.1 ± 18.1[a]	49.6 ± 18.6[a]	0.4 ± 0.2	3.3 ± 0.2

[a]Indicates $P < 0.05$ compared with Non-TP group.

TABLE IV. The Pathological Findings of the Liver for Each Group

	Control		Groups					
			1W		2W		3W	
Cirrhosis stage	Normal	CCl_4 9W	Non-TP	TP	Non-TP	TP	Non-TP	TP
0	6	0	0	0	0	1	0	0
1	0	0	0	0	0	0	0	0
2	0	0	1	0	0	1	0	0
3	0	0	3	6	3	4	3	6
4	0	6	2	0	3	0	4	0

The grade of CCl_4-injured rat livers scored by histopathological criteria, modified from Nanji et al. [1989] 0–4 as follows: 0 representing no fibrosis, 1 representing fibrosis confined to enlarged portal zones, 2 representing periportal or portal-portal septa with intact architecture, 3 representing architectural distortion (septal fibrosis, bridging) without obvious cirrhosis, and 4 representing probable or definite cirrhosis.

Stem cells have great potential as a therapeutic intervention in the treatment of degenerative diseases that affect various tissues, including the liver [Daley and Scadden, 2008]. Their therapeutic effects may be influenced by numerous factors such as cell count, differentiation potential, transplant method, and disease model [Petersen et al., 1999; Huttmann et al., 2003; Kuo et al., 2008]. BM-

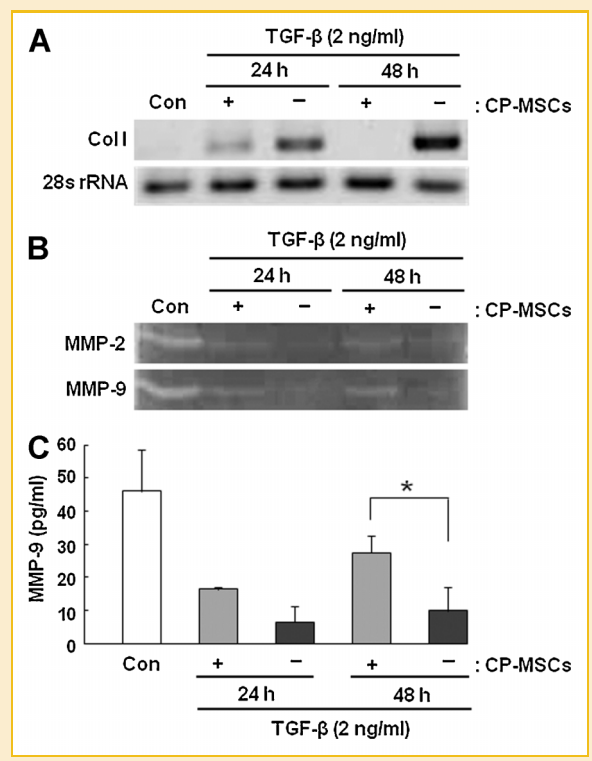

Fig. 7. Effects of CP-MSCs co-culture on collagen synthesis in a hepatic stellate cell line (T-HSC/C16) exposed to TGF-β. Synthesis of Col I increased in T-HSC/Cl-6 cells exposed to TGF-β (2 ng/ml) at 24 and 48 h. A: Co-culture of CP-MSCs with T-HSC/Cl-6 exposed to TGF-β (2 ng/ml) inhibited Col I synthesis at 24 and 48 h. B: Enzyme activity of MMP-2 and MMP-9 in co-cultured medium was analyzed by zymography. C: Quantitative amounts of MMP-9 in co-cultured medium were analyzed by ELISA assay. * indicates $P < 0.05$. Con, control (T-HSC/Cl-6 without TGF-β treatment).

MSCs have been touted as a potential source of hepatic oval cells, which are involved in liver regeneration [Petersen et al., 1999; Schmelzer et al., 2007]. Zhao et al. [2005] reported that BM-MSCs can engraft into injured tissues of bone marrow, lung, liver, heart, and brain, and facilitate the recovery of tissue function by reducing inflammation and remodeling the tissue. Although a significant reduction of liver fibrosis was observed in CCl_4-injured rats treated with BM-MSCs [Sakaida et al., 2005], the mechanism by which MSCs repair fibrosis remains unclear. Reports have variously claimed that BM-MSCs have no effect on liver injury in a rat model [Carvalho et al., 2008], can transform into fibrogenic liver cells [Higashiyama et al., 2007], and are associated with the development of cancer [Chakraborty et al., 2004; Yilmaz et al., 2005]. Elsewhere, MSCs derived from umbilical cord have shown therapeutic potential in a rat liver fibrosis model [Jung et al., 2009; Tsai et al., 2009].

In contrast, the therapeutic effects of CP-MSCs in CCl_4-injured rats have not been explored. CP-MSCs, organ-specific PDSCs derived from fetuses, are primitive intermediates between embryonic and adult stem cells. Although a basic characterization of PDSCs and an analysis of their differentiation potential have been reported [Parolini et al., 2008], few data describe their therapeutic potential. Interestingly, in the present study, undifferentiated CP-MSCs were found to express stem cell markers and three germ layer markers, as well as albumin. These characteristics indicate that CP-MSCs may help to heal damaged hepatocytes and improve the function of the injured liver through anti-fibrotic effects, suggesting their potential use in cell-based liver disease therapies.

Histopathological improvements in the CCl_4-injured liver in the rats transplanted with CP-MSCs may be linked to the observed improvement in function of the damaged liver (Table III, Fig. 6B), as well as the decreased deposition of collagen (Table IV, Fig. 6). The mechanism by which transplanted CP-MSCs inhibit collagen deposition in injured liver tissue may involve the induction of MMP expression. We confirmed that CP-MSCs inhibit collagen synthesis, trigger the expression of MMPs, and modulate MMP activities in TGF-β-exposed T-HSC/Cl-6 cells in an in vitro co-culture system (Fig. 7). These results are similar to those of previous reports, which have shown that transplanted BM-MSCs increase MMP expression in liver failure models [Sakaida et al., 2004; Higashiyama et al., 2007]. Furthermore, Cargnoni et al. [2009] reported that transplantation of allogenic and xenogenic PDSCs reduced both neutrophil infiltration and fibrosis in mice with bleomycin-induced lung fibrosis within 2 weeks. These reports suggest the possibility that PDSCs may be useful therapeutic reagents in the treatment of degenerative diseases characterized by abnormal collagen deposition. Our own studies demonstrating the anti-fibrotic effects of CP-MSCs on TGF-β-exposed T-HSC/Cl-6 cells support this hypothesis.

In the present study, the results of ICG uptake and excretion assays in CCl_4-injured rats suggest that the physiological function of damaged liver tissues may be restored by engrafted CP-MSCs. In addition, ICG uptake and excretion assays themselves may be useful tools for establishing the extent of spontaneous recovery from liver injury in model animals as well as in clinical medicine [Yamada et al., 2002]. Using these tools to analyze hepatic function, we confirmed the improvement of hepatic function following the transplantation of CP-MSCs into the CCl_4-injured rats. However, we evaluated the therapeutic potential of only one cell dose (2×10^6) and one transplantation route (direct transplant into liver). To improve the therapeutic effects of CP-MSCs, future studies should attempt to determine the optimum number of cells for promoting target organ function following transplantation and to identify the most effective transplantation routes. In addition, the therapeutic effects of CP-MSCs in CCl_4-injured rats should be studied for a longer time after CP-MSC transplantation.

In conclusion, we demonstrated that CP-MSCs can differentiate into functional hepatocyte-like cells in vitro and, when transplanted into CCl_4-injured rat livers, can improve hepatic function by inhibiting collagen synthesis and deposition. This study furthers our understanding of the pathophysiological roles of CP-MSCs in liver diseases and provides a foundation for the potential development of new therapeutic strategies for difficult-to-treat liver diseases.

ACKNOWLEDGMENTS

We thank Kyung-Seon Shin and Ji-Ye Song for technical supports of the animal experiment and special thank Dr. Seh-Hoon Oh (University of Florida College of Medicine, USA) for critical comments of the manuscript. This work was supported by the Korea Healthcare technology R&D Project, Ministry for Health Welfare & Family Affairs, Republic of Korea (A084633).

REFERENCES

Bailo M, Soncini M, Vertua E, Signoroni PB, Sanzone S, Lombardi G, Arienti D, Calamani F, Zatti D, Paul P, Albertini A, Zorzi F, Cavagnini A, Candotti F, Wengler GS, Parolini O. 2004. Engraftment potential of human amnion and chorion cells derived from term placenta. Transplantation 78:1439–1448.

Barlow S, Brooke G, Chatterjee K, Price G, Pelekanos R, Rossetti T, Doody M, Venter D, Pain S, Gilshenan K, Atkinson K. 2008. Comparison of human placenta- and bone marrow-derived multipotent mesenchymal stem cells. Stem Cells Dev 17:1095–1107.

Berg CL, Gillespie BW, Merion RM, Brown RS, Jr., Abecassis MM, Trotter JF, Fisher RA, Freise CE, Ghobrial RM, Shaked A, Fair JH, Everhart JE. 2007. Improvement in survival associated with adult-to-adult living donor liver transplantation. Gastroenterology 133:1806–1813.

Cargnoni A, Gibelli L, Tosini A, Signoroni PB, Nassuato C, Arienti D, Lombardi G, Albertini A, Wengler GS, Parolini O. 2009. Transplantation of allogeneic and xenogeneic placenta-derived cells reduces bleomycin-induced lung fibrosis. Cell Transplant 18:405–422.

Carvalho AB, Quintanilha LF, Dias JV, Paredes BD, Mannheimer EG, Carvalho FG, Asensi KD, Gutfilen B, Fonseca LM, Resende CM, Rezende GF, Takiya CM, de Carvalho AC, Goldenberg RC. 2008. Bone marrow multipotent mesenchymal stromal cells do not reduce fibrosis or improve function in a rat model of severe chronic liver injury. Stem Cells 26:1307–1314.

Chakraborty A, Lazova R, Davies S, Backvall H, Ponten F, Brash D, Pawelek J. 2004. Donor DNA in a renal cell carcinoma metastasis from a bone marrow transplant recipient. Bone Marrow Transplant 34:183–186.

Chang CJ, Yen ML, Chen YC, Chien CC, Huang HI, Bai CH, Yen BL. 2006. Placenta-derived multipotent cells exhibit immunosuppressive properties that are enhanced in the presence of interferon-gamma. Stem Cells 24: 2466–2477.

Chang CM, Kao CL, Chang YL, Yang MJ, Chen YC, Sung BL, Tsai TH, Chao KC, Chiou SH, Ku HH. 2007. Placenta-derived multipotent stem cells induced to differentiate into insulin-positive cells. Biochem Biophys Res Commun 357:414–420.

Constandinou C, Henderson N, Iredale JP. 2005. Modeling liver fibrosis in rodents. Methods Mol Med 117:237–250.

Costa RH, Grayson DR. 1991. Site-directed mutagenesis of hepatocyte nuclear factor (HNF) binding sites in the mouse transthyretin (TTR) promoter reveal synergistic interactions with its enhancer region. Nucleic Acids Res 19:4139–4145.

Crawford JM. 1999. Pathologic basis of disease: The liver and biliary tract. Philadelphia, PA: Saunders. pp. 845–891.

Daley GQ, Scadden DT. 2008. Prospects for stem cell-based therapy. Cell 132:544–548.

Di Bisceglie AM, Carithers RL, Jr., Gores GJ. 1998. Hepatocellular carcinoma. Hepatology 28:1161–1165.

Hay DC, Zhao D, Fletcher J, Hewitt ZA, McLean D, Urruticoechea-Uriguen A, Black JR, Elcombe C, Ross JA, Wolf R, Cui W. 2008. Efficient differentiation of hepatocytes from human embryonic stem cells exhibiting markers recapitulating liver development in vivo. Stem Cells 26:894–902.

Higashiyama R, Inagaki Y, Hong YY, Kushida M, Nakao S, Niioka M, Watanabe T, Okano H, Matsuzaki Y, Shiota G, Okazaki I. 2007. Bone marrow-derived cells express matrix metalloproteinases and contribute to regression of liver fibrosis in mice. Hepatology 45:213–222.

Huttmann A, Li CL, Duhrsen U. 2003. Bone marrow-derived stem cells and ''plasticity''. Ann Hematol 82:599–604.

In 't Anker PS, Scherjon SA, Kleijburg-van der Keur C, de Groot-Swings GM, Claas FH, Fibbe WE, Kanhai HH. 2004. Isolation of mesenchymal stem cells of fetal or maternal origin from human placenta. Stem Cells 22:1338–1345.

Iredale JP. 2007. Models of liver fibrosis: Exploring the dynamic nature of inflammation and repair in a solid organ. J Clin Invest 117:539–548.

Jung KH, Shin HP, Lee S, Lim YJ, Hwang SH, Han H, Park HK, Chung JH, Yim SV. 2009. Effect of human umbilical cord blood-derived mesenchymal stem cells in a cirrhotic rat model. Liver Int 29:898–909.

Kaimori A, Potter J, Kaimori JY, Wang C, Mezey E, Koteish A. 2007. Transforming growth factor-beta1 induces an epithelial-to-mesenchymal transition state in mouse hepatocytes in vitro. J Biol Chem 282:22089–22101.

Kuo TK, Hung SP, Chuang CH, Chen CT, Shih YR, Fang SC, Yang VW, Lee OK. 2008. Stem cell therapy for liver disease: Parameters governing the success of using bone marrow mesenchymal stem cells. Gastroenterology 134:2111–2121 e1–3.

Lee GP, Jeong WI, Jeong DH, Do SH, Kim TH, Jeong KS. 2005. Diagnostic evaluation of carbon tetrachloride-induced rat hepatic cirrhosis model. Anticancer Res 25:1029–1038.

Nanji AA, Mendenhall CL, French SW. 1989. Beef fat prevents alcoholic liver disease in the rat. Alcohol Clin Exp Res 13:15–19.

Oyagi S, Hirose M, Kojima M, Okuyama M, Kawase M, Nakamura T, Ohgushi H, Yagi K. 2006. Therapeutic effect of transplanting HGF-treated bone marrow mesenchymal cells into CCl4-injured rats. J Hepatol 44:742–748.

Parolini O, Alviano F, Bagnara GP, Bilic G, Buhring HJ, Evangelista M, Hennerbichler S, Liu B, Magatti M, Mao N, Miki T, Marongiu F, Nakajima H, Nikaido T, Portmann-Lanz CB, Sankar V, Soncini M, Stadler G, Surbek D, Takahashi TA, Redl H, Sakuragawa N, Wolbank S, Zeisberger S, Zisch A, Strom SC. 2008. Concise review: Isolation and characterization of cells from human term placenta: Outcome of the first international Workshop on Placenta Derived Stem Cells. Stem Cells 26:300–311.

Perkins JD. 2007. Quality of life after liver transplantation for acute hepatic failure. Liver Transpl 13:1604–1605.

Petersen BE, Bowen WC, Patrene KD, Mars WM, Sullivan AK, Murase N, Boggs SS, Greenberger JS, Goff JP. 1999. Bone marrow as a potential source of hepatic oval cells. Science 284:1168–1170.

Sakaida I, Terai S, Yamamoto N, Aoyama K, Ishikawa T, Nishina H, Okita K. 2004. Transplantation of bone marrow cells reduces CCl4-induced liver fibrosis in mice. Hepatology 40:1304–1311.

Sakaida I, Terai S, Nishina H, Okita K. 2005. Development of cell therapy using autologous bone marrow cells for liver cirrhosis. Med Mol Morphol 38:197–202.

Schmelzer E, Zhang L, Bruce A, Wauthier E, Ludlow J, Yao HL, Moss N, Melhem A, McClelland R, Turner W, Kulik M, Sherwood S, Tallheden T, Cheng N, Furth ME, Reid LM. 2007. Human hepatic stem cells from fetal and postnatal donors. J Exp Med 204:1973–1987.

Stolzing A, Jones E, McGonagle D, Scutt A. 2008. Age-related changes in human bone marrow-derived mesenchymal stem cells: Consequences for cell therapies. Mech Ageing Dev 129:163–173.

Talens-Visconti R, Bonora A, Jover R, Mirabet V, Carbonell F, Castell JV, Gomez-Lechon MJ. 2007. Human mesenchymal stem cells from adipose tissue: Differentiation into hepatic lineage. Toxicol In Vitro 21:324–329.

Tsai PC, Fu TW, Chen YM, Ko TL, Chen TH, Shih YH, Hung SC, Fu YS. 2009. The therapeutic potential of human umbilical mesenchymal stem cells from Wharton's jelly in the treatment of rat liver fibrosis. Liver Transpl 15:484–495.

Yamada T, Yoshikawa M, Kanda S, Kato Y, Nakajima Y, Ishizaka S, Tsunoda Y. 2002. In vitro differentiation of embryonic stem cells into hepatocyte-like cells identified by cellular uptake of indocyanine green. Stem Cells 20:146–154.

Yilmaz Y, Lazova R, Qumsiyeh M, Cooper D, Pawelek J. 2005. Donor Y chromosome in renal carcinoma cells of a female BMT recipient: Visualization of putative BMT-tumor hybrids by FISH. Bone Marrow Transplant 35:1021–1024.

Zhao DC, Lei JX, Chen R, Yu WH, Zhang XM, Li SN, Xiang P. 2005. Bone marrow-derived mesenchymal stem cells protect against experimental liver fibrosis in rats. World J Gastroenterol 11:3431–3440.